ELSEVIER

Coordination Chemistry Reviews
219–221 (2001) 125–155

COORDINATION CHEMISTRY REVIEWS

www.elsevier.com/locate/ccr

Phenylcyanamide ligands and their metal complexes

Robert J. Crutchley *

Ottawa-Carleton Chemistry Institute, Carleton University, 1125 Colonel By Drive, Ottawa, Ontario, Canada K1S 5B6

Received 31 August 2000; received in revised form 14 November 2000; accepted 19 December 2000

Dedicated to Professor A.B.P. Lever

Contents

* Tel.: +1-613-520-2600 ext. 3848; fax: +1-613-520-3749.
E-mail address: robert_crutchley@carleton.ca (R.J. Crutchley).

PII: S0010-8545(01)00324-1

Abstract

This review examines the various synthetic routes to phenylcyanamide ligands, and their physical characterization by electronic, NMR and IR spectroscopies, crystallography and theoretical methods. While the coordination chemistry of phenylcyanamide ligands is largely unexplored, a significant number of mononuclear coordination complexes of ruthenium, copper and nickel group ions have been synthesized. Topics to be covered are UV–vis, NMR and IR spectroscopy, linkage isomerism and crystallography, and finally cyclic voltammetry. Studies of the remarkable ability of the 1,4-dicyanamidobenzene dianion bridging ligand to mediate antiferromagnetic or resonance exchange in dinuclear ruthenium complexes will be reviewed.

Keywords: Phenylcyanamide; Charge transfer; Mixed-valence; Electron exchange

1. Introduction

The coordination chemistry of phenylcyanamide ligands is expected to be as potentially rich as that of the pseudohalides (for example, azide [1] or thiocyanate [2]). However, very little has been done and it is only through recent efforts that this chemistry is being elucidated. The attachment of a phenyl ring to the cyanamide group adds an extra dimension not present in azide or thiocyanate ligands. An extensive π conjugation between the cyanamide group and the phenyl ring provides an energetically favorable means by which a metal ion can couple into a conjugated organic π system. This is demonstrated in this review by the extraordinary ability of 1,4-dicyanamidobenzene to mediate metal–metal coupling, the magnitude of which is dramatically dependent upon the nature of both inner and outer coordination spheres. The wealth of data provided by the study of these dinuclear systems has permitted a quantitative evaluation of metal–metal coupling within the context of Marcus–Hush theory [3] and the determination of metal–metal and metal–ligand coupling elements using charge-transfer band oscillator strengths [4]. The recent interest in the field of inorganic chemistry to develop novel hybrid materials that combine coordination and organic chemistry provides further impetus to this research.

2. Synthesis of phenylcyanamide derivatives

2.1. Neutral phenylcyanamides (pcydH)

Phenylcyanamide derivatives can be readily prepared in high yields from the corresponding anilines [5,6]. An aniline is reacted with benzoylthiocyanate in acetone to generate the benzoylthiourea. This is isolated and hydrolyzed in aqueous solution to form the thiourea, which is then desulfurized using Pb(II), as shown in Scheme 1.

Lead sulfide is filtered off and to the filtrate glacial acetic acid is added, precipitating the neutral phenylcyanamide. The above reaction does not appear to be particularly limited by the number and type of substituents as polychloro, -fluoro, -methyl and -methoxy substituted phenylcyanamides have been successfully synthesized. Experience has shown that there are three elements to a successful synthesis. First, hydrolysis of the benzoylthiourea is usually complete after the alkaline aqueous solution is boiled for 10 min. Second, desulfurization by Pb(II) should be performed at temperatures not greater than 65°C and finally precipitation of the cyanamide by protonation should be done as quickly as possible.

A number of phenylcyanamide derivatives, particularly the *ortho*-substituted polyhalides, were subjected to a dimerization reaction, forming *N*-phenyl-*N′*-cyano-*N′*-phenyl-guanidine derivatives [7](Scheme 2).

For example, 2,6-dichlorophenylcyanamide in DMSO was observed by ^{1}H-NMR to dimerize within a few hours [7]. This reaction could be suppressed by the addition of acid, suggesting that the mechanism is deprotonation followed by attack of the amide on the nitrile carbon of a neutral ligand. The dimer is colorless like the monomer and has similar solubility in non-aqueous solvents. The presence of the dimer can be recognized by IR spectroscopy as its strong ν(C=N) band at ca. 1670 cm^{-1} is absent in the monomer.

The following 1,4-dicyanamidebenzenes (dicydH_2) have been synthesized from phenylenediamines by the desulfurization of thiourea method [8,9], 2,3,5,6-tetra-chloro-, 2,5-dichloro-, 2-chloro-, 2-methyl, 2-methoxy-, 2,5-dimethyl-, 2,3,5,6-te-tramethyl- and unsubstituted 1,4-dicyanamidebenzene. 1,3-Dicyanamidebenzene can also be prepared but the 1,2-dicyanamide isomer cannot [10]. In the latter

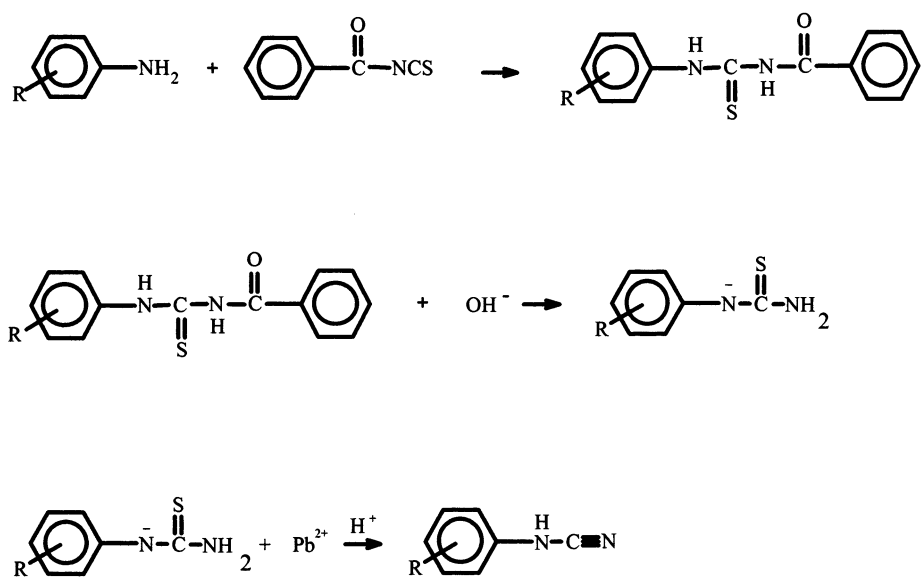

Scheme 1.

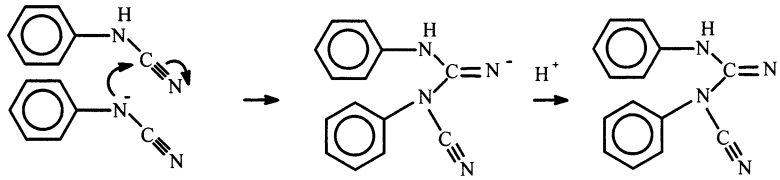

Scheme 2.

attempt, a large quantity of thiocyanate was found in the filtrate after desulfurization. This suggests that the anionic thiourea groups must undergo an elimination step. The thiourea method was also used to prepare 4,4′-dicyanamidebiphenyl [11].

Phenylcyanamides can be recrystallized in high yields from boiling acetone–water solutions. The procedure is usually to dissolve the phenylcyanamide in boiling acetone and while maintaining the temperature, add water until the solution just becomes cloudy. Crystals of the product are formed from the cooling solution. Methanol and ethanol have been used in place of acetone with good results in some instances.

Other researchers have synthesized phenylcyanamides by the reaction of phenylisocyanide dihalides with ammonia [12], or by the reaction of anilines with cyanogen bromide [13]. A recently prepared cyanating agent, *N′*-cyanoimidazole, when reacted with aniline yielded phenylcyanamide in high yields under moderate conditions [14]. The latter reaction may provide a route to more sensitive cyanamide derivatives.

2.2. Anionic phenylcyanamides (pcyd$^-$)

Thallium salts of anionic phenylcyanamides can be prepared from either the monomer or the dimer phenylcyanamide derivatives in acetone–water, in the presence of triethylamine (TEA) [6](Scheme 3).

Thallium salts derived from dimeric phenylcyanamides no longer have an imine stretch in their IR spectra. These spectra are identical to those of the thallium salts of monomeric phenylcyanamides [7]. The white thallium salts of phenylcyanamide ligands are not very soluble in non-aqueous solutions at room temperature and the toxicity of thallium is a concern. Ag(I) is a possible substitute for Tl(I) [5]. However, the photosensitivity and oxidation properties of silver salts make its use less desirable.

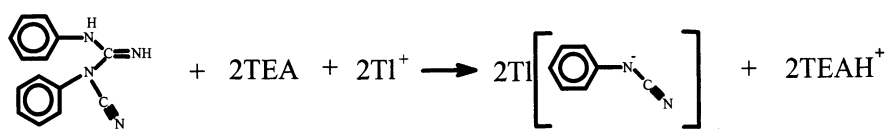

Scheme 3.

The lithium salt of phenylcyanamide was prepared by deprotonation of 5-(phenylamino)-1,2,3,4-thiatriazole with various lithium bases [15]. A crystal structure of the product showed a linear chain structure in which the cyanamide groups are coordinated to lithium cations through both their amide and cyano-nitrogens. This type of coordination mode has been seen in Cu(II) complexes and will be discussed in Sections 4.1 and 4.6.

The 1,4-dicyanamidebenzene dianion and its substituted derivatives can be precipitated from acetone solution as yellow thallium salts by using the above reaction [16]. The thallium salts are slightly air sensitive, turning slightly green upon oxidation, and should be stored under argon. Tetraphenylarsonium salts have greater solubility in non-aqueous solvents than the Tl(I) salts and have been used to grow X-ray quality crystals [17]. These salts appear more air-sensitive than their thallium analogues.

3. Physical properties of phenylcyanamides

The cyanamide group is a three-atom π-system in which the amine non-bonding electrons can delocalize into the nitrile π-bonds. Accordingly, the cyanamide group is expected to be a poorer π-acceptor but better donor than analogous nitrile ligands [18]. For this reason, cyanamides are expected to be less sensitive to base hydrolysis. The extent of delocalization of the amine lone pair into the phenyl group is influenced by the nature and the number of phenyl ring substitutents. Table 1 gives ^{13}C-NMR and IR spectroscopic data and melting points for 14 phenylcyanamide derivatives. The numbering scheme for ^{13}C-NMR data and pcyd$^-$ derivatives is shown below

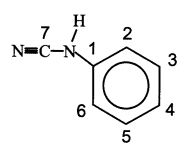

A ^{15}N-NMR study of phenylcyanamides has also been performed [19]. The ν(NCN) of the phenylcyanamides (Table 1) varies very little (2225–2249 cm^{-1}) but the overall trend is consistent with the nature of the phenyl ring substituents.

The amine proton of phenylcyanamide is relatively acidic compared to other secondary amines and this is because of a resonance stabilization of the negative charge

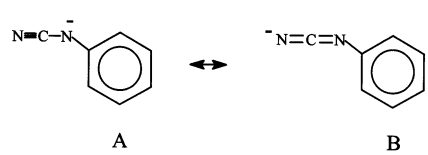

Table 1
^{13}C-NMR, [a] IR [b] spectroscopic data and melting points [c] of substituted phenylcyanamide ligands (pcydH)

Ligands	^{13}C-NMR							IR ν(NCN)	Melting point (°C)
	C_1	C_2	C_3	C_4	C_5	C_6	C_7		
2,4,6-Me_3pcydH [d]	134.2	131.0	128.3	130.6	128.3	131.0	113.4	2225	102
3,5-Me_2pcydH [e]	137.4	111.6	138.0	123.1	138.0	111.6	111.1	2239	124
4-MepcydH [f]	135.1	113.9	129.1	130.4	129.1	113.9	111.3	2227	62
3,4,5-MeO_3pcydH [g]	132.9	92.7	153.8	134.9	153.8	92.7	112.2	2220	113
3,5-MeO_2pcydH [h]	94.5	93.6	161.5	139.3	161.5	93.6	111.9	2229	150
pcydH	136.9	113.3	128.0	120.9	128.0	113.8	108.7	2227	34
2-ClpcydH	132.5	117.2	127.2	121.1	125.7	113.8	108.8	2243	109
3-ClpcydH	138.9	113.4	132.8	121.0	129.8	112.2	109.9	2237	101
4-ClpcydH	136.3	115.2	128.0	125.0	128.0	115.2	110.3	2232	106
2,3-Cl_2pcydH	136.5	114.1	128.0	123.3	131.7	117.5	110.2	2235	156
2,4-Cl_2pcydH	133.2	119.4	127.9	125.6	127.0	116.3	109.8	2235	170
2,6-Cl_2pcydH	133.0	129.1	130.2	128.2	130.2	129.1	112.1	2249	120 [i]
2,4,5-Cl_3pcyd	134.2	113.9	129.2	123.6	129.4	115.6	109.1	2245	170
2,3,4,5-Cl_4pcydH	135.4	117.6	131.1	122.9	130.2	114.0	108.0	2243	168 [i]

[a] In dimethylsulfoxide and referenced to DMSO's methyl resonance at 39.5 ppm, at ambient temperature, from Ref. [30].
[b] Nujols mulls, very strong bands, in cm^{-1}.
[c] Phenylcyanamides polymerize when heated slowly.
[d] Methyl groups on C_2 and C_6, 16.9 ppm and methyl group on C_4, 19.3 ppm.
[e] Methyl groups on C_3 and C_5, 19.8 ppm.
[f] Methyl group on C_4, 19.2 ppm.
[g] Methoxy groups on C_3 and C_5, 55.8 ppm and methoxy group on C_4, 60.1 ppm.
[h] Methoxy groups on C_3 and C_5, 55.2 ppm.
[i] Initial melting was followed by solidification.

For example, the pK_a of 2,6-dichlorophenylcyanamide was measured at 4.90 ± 0.05 [7]. Deprotonation of the cyanamide group shifts ν(NCN) to lower frequencies (ca. 2120 cm^{-1}) similar to that of organic carbodiimides (for R–N=C=N–R, ν(NCN) ranges from 2100–2150 cm^{-1}) [20]. This suggests that resonance form **B** makes the dominant contribution to the cyanamide anion group as resonance form **A** should have a nitrile stretching frequency similar to neutral cyanamide. Extended Hückel calculations gave two π_{nb} orbitals in C_s symmetry, which result from the delocalization of nonbonding electrons of the cyanamide group into the phenyl ring [21]. The calculations showed that the π_{nb2} symmetry orbital is more stable than the π_{nb1} symmetry orbital by 0.49 eV.

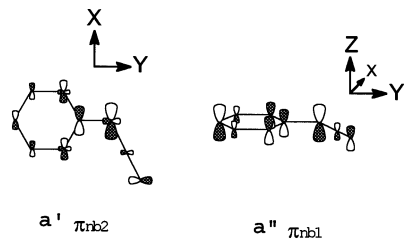

Crystal structures of 2,3,4,5-tetrachloro- (Cl_4dicyd^{2-}) [22], 2,5-dichloro- (Cl_2dicyd^{2-}) [17], 2,5-dimethyl- (Me_2dicyd^{2-}) [17], 2,3,5,6-tetramethyl- (Me_4dicyd^{2-}) [23] and 1,4-dicyanamidebenzene dianion ($dicyd^{2-}$) [17] have been published. A representative crystal structure of the 1,4-dicyanamidebenzene dianion ($dicyd^{2-}$) is shown in Fig. 1. Except for the tetramethyl derivative, all of the dianion ligands are approximately planar with cyanamide groups in an *anti*-conformation. Planarity of the phenylcyanamide ligand optimizes the π interaction between the phenyl ring and the cyanamide groups. In the case of the tetramethyl-substituted derivative, steric repulsion between the *ortho*-methyl groups and the cyanamide groups is enough to force the cyanamide groups out of the phenyl ring plane while still maintaining an *anti* conformation [23]. A crystal structure was also performed on the air stable tetraphenylarsonium salt of 4,4′-dicyanamidebiphenyl dianion [11]. The dianion adopts an approximately planar geometry and, despite

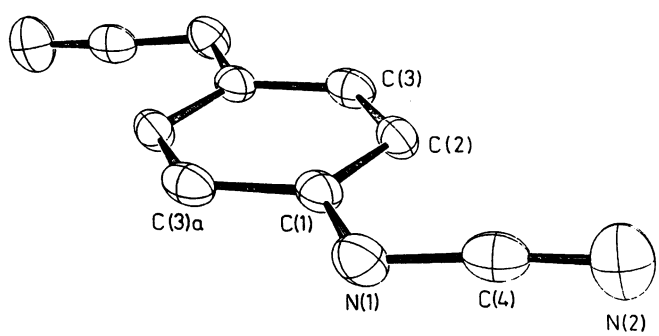

Fig. 1. ORTEP drawing of the 1,4-dicyanamidebenzene dianion ($dicyd^{2-}$).

steric repulsion between the *ortho*-hydrogens, possesses a dihedral angle of only 8.2° between the phenyl rings. The above crystal structure observations have important consequences to metal–metal coupling as will be discussed later.

The anionic cyanamide groups of dicyd^{2-} (Fig. 1) are approximately linear with the NCN angle of 174.1(6)° [17]. The terminal nitrogen to carbon bond length is 1.172(10) Å, showing significant triple bond character, and the carbon to amide nitrogen bond length is 1.299(10) Å, showing significant double bond character. This indicates that the bond lengths of the cyanamide group are not simply the average of resonance forms **A** and **B** and suggest that carbon in cyanamide possesses hypervalent character. Substituted derivatives of dicyd^{2-} possess similar cyanamide group bond lengths and angles [17,22,23].

Anionic phenylcyanamides do not have well-behaved cyclic voltammetry and generally give an irreversible oxidation wave [6]. However, 1,4-dicyanamidebenzene dianion ligands do give reversible oxidation waves with electrochemistry analogous to that of the quinone/hydroquinone system [24]. The reduction couples are shown below Scheme 4

The corresponding cyclic voltammetry data of 1,4-dicyanamidebenzene derivatives so far used in coordination chemistry are found in Table 2. A more extensive investigation of the electrochemistry of *N*,*N*′-dicyanoquinonediimine derivatives (L^0) has been reported [25]. The dianion is very unstable and readily oxidizes to the blue radical anion in the presence of oxygen. This is illustrated by Fig. 2, which shows the spectroelectrochemical oxidation of 1,4-dicyanamidebenzene dianion [26]. *N*,*N*′-dicyanoquinonediimine derivatives have been used to make conducting organic and organo-metallic charge-transfer salts [27]. Indeed, the copper salt of the radical anion of 2,5-dimethyl-*N*,*N*′-dicyanoquinonediimine exhibited metallic conductivity down to 3.5 K with $\sigma = 500\,000$ S cm^{-1} [28].

$$L^- + e^- \rightleftharpoons L^{2-} \quad L(-/2-)$$
$$L^0 + e^- \rightleftharpoons L^- \quad L(0/-)$$

Scheme 4.

Table 2
Cyclic voltammetry data of 1,4-dicyanamidebenzene dianion (dicyd^{2-}) and its derivatives in acetonitrile (data are in V versus NHE (internal calibrant was ferrocene, $E° = 0.665$ versus NHE), 0.1 M tetrabutylammonium hexafluorophosphate, from Ref. [8])

Species	L(−/2−)	L(0/−)
Dicyd^{2-}	−0.200	0.475
Me_2dicyd^{2-}	−0.280	0.360
Me_4dicyd^{2-}	−0.300	0.195
Cl_2dicyd^{2-}	0.090	0.730
Cl_4dicyd^{2-}	0.240	0.835

4. Coordination chemistry of phenylcyanamides

4.1. Coordination geometry

The phenylcyanamides are ambidentate ligands whether neutral or in anionic form and so the possibility of linkage isomerism must be recognized. As shown below, neutral phenylcyanamides can coordinate to a metal ion through either the nitrile or the amine nitrogen. However, at this point in time, there are no crystal structures of neutral phenylcyanamides coordinated to metal ions. The amine nitrogen is sterically crowded by the phenyl ring and so terminal coordination to the nitrile is expected, particularly for electron-rich metal centers. Metal ions that behave as π-acceptors are expected to favor the anionic phenylcyanamide ligand in order to take advantage of the ligand's π-donor properties. In this regard, the pK_a of neutral 2,6-dichlorophenylcyanamide coordinated to Ru(III) was determined to be 0.93 ± 0.05, a 3.97 pH shift relative that of its free ligand. For this neutral ligand coordinated to Ru(II), its pK_a was calculated to be 7.13, a 6.2 pH unit shift in acidity of the coordinated phenylcyanamide ligand upon a single unit change in oxidation state [7]. Side-on coordination of the cyanamide group has not been observed for phenylcyanamide ligands but has been observed in tungsten complexes of dialkylcyanamides [29].

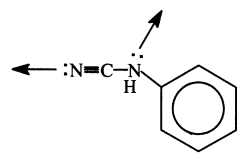

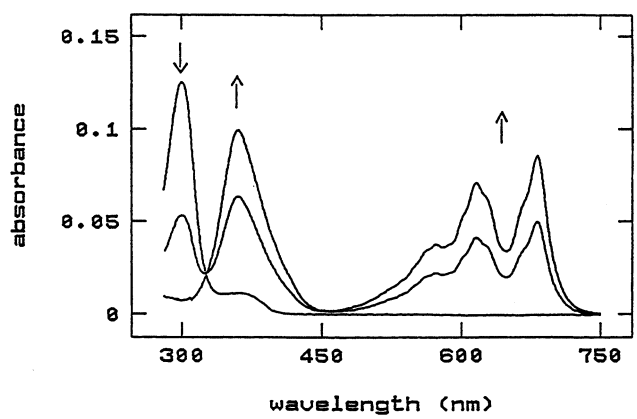

Fig. 2. Spectroelectrochemical oxidation of $[AsPh_4]_2$[dicyd], 4.63×10^{-6} M in acetonitrile, forming the radical anion, 0.1 M TBAH, from Ref. [26] and reproduced with permission from the American Chemical Society.

Anionic phenylcyanamides have three non-bonding pairs of electrons that can be involved in coordination chemistry, as shown below

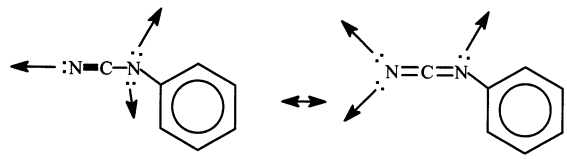

A B

There are many crystal structures of monodentate phenylcyanamide ligands showing coordination through the cyano-nitrogen but there are no examples of amide-nitrogen coordination. The neutral or anionic phenylcyanamides can function as bridging ligands although this has only been observed for the anionic cyanamide

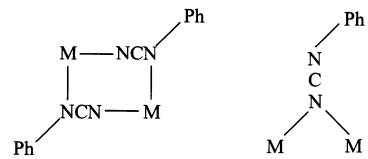

I II

Both bridging modes I and II have been observed in copper(II) complexes and will be discussed in Section 4.5.

4.2. Complex synthesis

The method one chooses depends upon the lability of the auxiliary ligands. For example, ammine ligands bonded to Ru(II) or Ru(III) are notoriously labile and reaction conditions must be moderate to ensure complex integrity. Thus, heating of the reaction mixture is avoided and product formation usually relies upon the inherent lability of the reagent complex as shown below (Scheme 5).

The initial reaction is performed under argon atmosphere and is followed by exposure to oxygen. Cation-exchange chromatography is almost always required to ensure complex purity [30]. This method has also been used to prepare the polyammine dinuclear ruthenium(III) complexes [8,9,31,32].

It is also possible to use thallium(I) salts of phenylcyanamide ligands and react them with complex halides in a metathesis reaction [5,33] (Scheme 6).

$$[Ru(NH_3)_5(OH_2)]^{2+} + pcydH \rightarrow [Ru(NH_3)_5(pcydH)]^{2+} + H_2O$$

$$[Ru(NH_3)_5(pcydH)]^{2+} + O_2 \rightarrow [Ru(NH_3)_5(pcyd)]^{3+} + O_2^- + H^+$$

Scheme 5.

$$Cu(bpy)_2Br^+ + Tl[pcyd] \rightarrow [Cu(bpy)_2(pcyd)]^+ + TlBr$$

$$[MCl_4]^{2-} + 4Tl[pcyd] \rightarrow [M(pcyd)_4]^{2-} + 4TlCl \quad M = Co(II), Ni(II), \text{and } Cu(II)$$

Scheme 6.

$$pcydH + Na[CH_3CH_2O] \rightarrow pcyd^- + Na^+ + CH_3CH_2OH$$

$$2[Cu(NCCH_3)_4]^+ + 3dppe + 2pcyd^- \rightarrow [Cu_2(dppe)_3(pcyd)_2]$$

Scheme 7.

The limiting factor for this reaction is the solubility of the thallous salt Tl[pcyd], which requires strong donor solvents and elevated temperatures. For these reasons, this reaction is most effective with substitutionally inert Ru(II) complexes and relies upon the irreversible formation of TlCl to drive itself to completion. Nevertheless, under mild conditions and low thallous salt solubility, this reaction can still prove successful provided the reaction time is sufficient.

Cu(I) complexes of phenylcyanamide ligands have been prepared by the deprotonation of phenylcyanamide with sodium ethoxide in acetone–ethanol and the addition of this solution to a solution of a Cu(I) reagent complex [34]. For example (Scheme 7).

4.3. Ruthenium complexes

4.3.1. Mononuclear ruthenium complexes

4.3.1.1. Neutral phenylcyanamides. Isolation of neutral phenylcyanamides bound to Ru(II) requires inert atmosphere techniques as the complexes readily oxidize. Only one complex, $[Ru(NH_3)_5(2,6\text{-}Cl_2pcydH)][PF_6]_2$, has been synthesized and was characterized by ^{1}H-NMR, IR and UV–vis spectroscopy, and cyclic voltammetry [7]. The UV–vis spectrum showed the presence of a new band that was not a ligand or metal-centered transition and was assigned to a Ru(II)-to-nitrile MLCT transition. This in turn suggests that the phenylcyanamide ligand is coordinated to Ru(II) through its cyano-nitrogens. This complex's IR spectrum was unusual in that its ν(NCN) was extremely weak when compared to the intensity the free ligand's ν(NCN). It was only by deuterating the complex and labeling the cyanamide with ^{15}N, that a weak peak at 2287 cm^{-1} could be assigned to ν(NCN). This band was shifted to higher frequencies by 38 cm^{-1} compared to the free ligand. The coordination of organonitrile ligands to pentaammineruthenium(II) has been shown to reduce the frequency of ν(CN) and has been ascribed to π-back bonding between Ru(II) and the π acceptor nitrile ligand [35]. When π back bonding is not important, as in pentaamminerhodium(III) organonitrile complexes [36] ν(CN) shifts to higher frequencies.

The Ru(III) complex, $[Ru(NH_3)_5(2,3\text{-}Cl_2pcydH)][ClO_4]_3$ has been prepared and characterized by IR, UV–vis spectroscopy and cyclic voltammetry [6]. This orange

perchlorate salt was found to be explosive and so extreme caution is advised. Fig. 3 shows the electronic absorption spectrum of this complex. The broad absorption centered at 487 nm has been assigned to the $b_2 \rightarrow b_2^*$, cyanamide-to-Ru(III) transition and is a consequence of the delocalization of the amine lone pair into the cyano-π bonds. This electronic transition also indicates that the neutral cyanamide group is a π-donor albeit weak. The IR spectrum of this complex showed a very strong band at 2287 cm^{-1} that was assigned to ν(NCN).

4.3.1.2. Anionic phenylcyanamides. There are many examples Ru(III) and Ru(II) phenylcyanamido complexes with the pentaammineruthenium(III) family comprising the largest number of complexes. $[Ru(NH_3)_5L]^{2+}$ complexes where L = 2,4,6-Me_3pcyd$^-$, 3,5-Me_2pcyd$^-$, 4-Mepcyd$^-$, 3,4,5-MeO_3pcyd$^-$, 3,5-MeO_2pcyd$^-$, pcyd$^-$, 3-Clpcyd$^-$, 2-Clpcyd$^-$, 4-Clpcyd$^-$, 2,3-Cl_2pcyd$^-$, 2,4-Cl_2pcyd$^-$, 2,6-Cl_2pcyd$^-$, 2,4,5-Cl_3pcyd$^-$, 2,4,6-Cl_3pcyd$^-$, 2,3,4,5-Cl_4pcyd$^-$, 2,3,5,6-Cl_4pcyd$^-$, and Cl_5pcyd$^-$, were characterized by IR and UV–vis spectroscopy and cyclic voltammetry [6,30]. An ORTEP drawing of $[Ru(NH_3)_5(2,3\text{-}Cl_2pcyd]^{2+}$ is shown in Fig. 4. Note again that the phenyl ring is approximately co-planar with the cyanamide group and that Ru(III)–NCN bond angle is approximately linear at 171.4(10)°. This geometry optimizes π-interactions and this will become more important in the discussion of dinuclear complexes and metal–metal coupling. Cyclic voltammetry data were calibrated using an old value for the ferrocenium/ferrocene couple, $Fc^+/Fc = 400$ mV versus NHE in acetontrile [37]. These should be corrected against the more recent value of $Fc^+/Fc = 665$ versus NHE [38]. For $[Ru(NH_3)_5L]^{2+}$, when L = 2,4,6-Me_3pcyd$^-$, the Ru(III/II) couple = −15 mV versus NHE while when L =

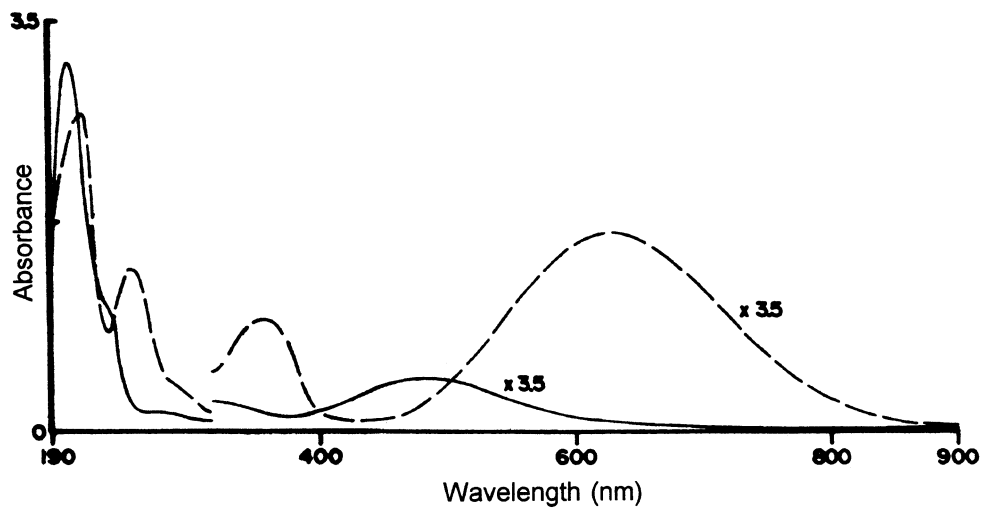

Fig. 3. UV–vis absorption spectra of $[Ru(NH_3)_5(2,3\text{-}Cl_2pcydH)]^{3+}$ in 2.5 M perchloric acid, (solid line) and $[Ru(NH_3)_5(2,3\text{-}Cl_2pcyd)]^{2+}$ in distilled water, pH 5.8 (dashed line), from Ref. [6] and reproduced with permission from the American Chemical Society.

Cl_5pycd^-, the Ru(III/II) couple = 229 mV versus NHE. Thus, the trend in Ru(III/II) couples [30] is consistent with the ability of the phenylcyanamide ligand to donate electron density.

Fig. 3 shows the quantitative electronic absorption spectrum of $[Ru(NH_3)_5(2,3\text{-}Cl_2pcyd)]^{2+}$ that is characteristic of the pentaammine family of complexes. The two bands centered at 356 and 629 nm have been assigned, assuming C_{2v} microsymmetry [6,21], to formally forbidden $b_2 \rightarrow b_1^*$ and allowed $b_1 \rightarrow b_1^*$ LMCT transitions, respectively, associated with the Ru(III)–cyanamide chromophore. The energy of the $b_1 \rightarrow b_1^*$ band (E_{max}) can be related to the difference between Ru(III/II) and L(0/−) couples according to [39,40]

$$E_{max} = [L(0/-) - Ru(III/II) + C] + \chi \quad (1)$$

where χ is the energy difference between an excited state at its zeroth vibrational level relative to the excited vibrational level populated during a Franck–Condon transition and C a correction term that takes into account solvation effects and reorganization energy.

It was also noted that the oscillator strength of the $b_1 \rightarrow b_1^*$ band varied depending upon the nature of the phenylcyanamide ligand and could be qualitatively related to the magnitude of the Ru(III/II)–cyanamide π bond overlap according to [30,41]

$$f = 1.085 \times 10^{-5} GvS^2R^2 \quad (2)$$

where G is the degeneracy of the transition, v the transition energy in cm^{-1}, S the overlap integral of a ruthenium dπ orbital with a cyanamide pπ orbital and R the transition dipole moment length. Mulliken [42,43], using the atomic orbital approximation, originally derived this equation for interatomic charge transfer between two totally symmetric hydrogen wavefunctions. The equation was an attempt to

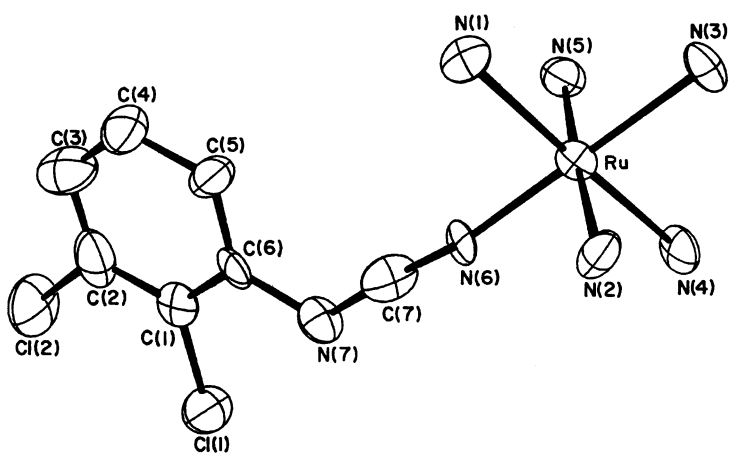

Fig. 4. ORTEP drawing of the complex cation, $[Ru(NH_3)_5(2,3\text{-}Cl_2pcyd)]^{2+}$, from Ref. [30] and reproduced with permission from the American Chemical Society.

explain the dependence of oscillator strength on the overlap of the wavefunctions involved in charge transfer and is applicable to a strong coupling case. If coupling between donor and acceptor is relatively weak, overlap can be neglected and this can result in more quantitative treatments [4]. This will be discussed for the dinuclear ruthenium complexes in Section 4.3.2.2.

The oscillator strength of the $b_1 \rightarrow b_1^*$ band also showed solvent-dependent behavior that could be related to the solvent donor number [30,44] as shown in Fig. 5. Pre-resonance Raman studies [45] of metal to ligand charge transfer in $[(NH_3)_4Ru(2,2'\text{-bipyridine})]^{2+}$ have provided direct evidence for the strengthening of the ammine nitrogen–ruthenium bond with increasing solvent donor number. The net effect of a hydrogen bond between solvent donor (:S) and ammine proton is the transfer of electron density from the partially deprotonated ammine to Ru(III).

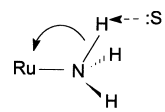

the limiting case being the complete loss of a proton and the formation of an amido ligand (a strong π donor). This sets up a competition with the cyanamide group for the πd orbitals, weakening the Ru(III)–cyanamide π-bond which in turn results in a decrease in the oscillator strength of the $b_1 \rightarrow b_1^*$ band.

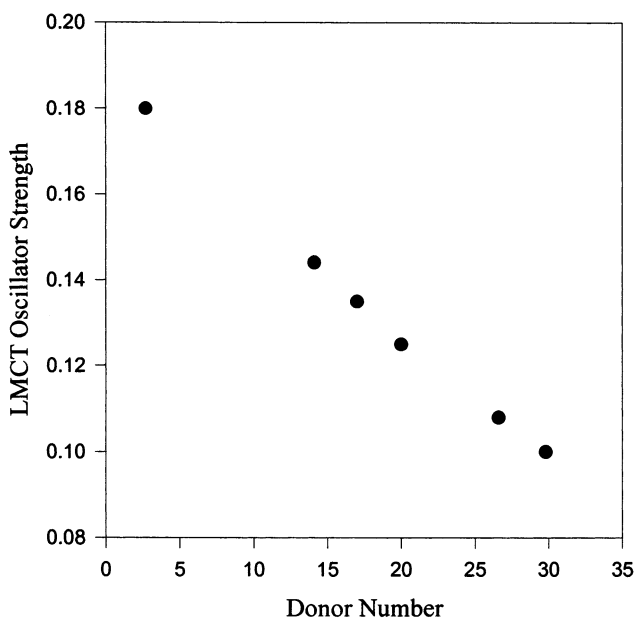

Fig. 5. Plot of the oscillator strength of the $b_1 \rightarrow b_1^*$ LMCT transition of $[(NH_3)_5Ru(2,3\text{-}Cl_2pcyd)][ClO_4]_2$ versus solvent donor number.

The effect of conjugation of the cyanamide ligand on the properties of the $b_1 \rightarrow b_1^*$ transition was studied by the synthesis and spectral characterization of $[Ru(NH_3)_5(NCNR)]^{2+}$ where NCNR is cyanamido, phenylcyanamido, 4-cyanamidobiphenyl, 1-cyanamidonaphthalene, 2-cyanamidonaphthalene, 2-cyanamidophenanthroline and 1-cyanamidopyrene [21]. The expected relationship between the transition dipole moment length and the oscillator strength (Eq. (2)) could only be qualitatively demonstrated by experiment.

Mononuclear complexes, $[(NH_3)_5Ru(LH)]^{2+}$ where $LH = Me_2dicydH^-$, dicydH$^-$ and Cl_2dicyd^-, have been prepared and characterized by electronic absorption spectroscopy and cyclic voltammetry [46]. These mononuclear complexes can be used as precusors to asymmetric dinuclear complexes and will be the subject of a future study [16].

When deprotonated, the complexes oxidize to the Ru(IV) oxidation state and this allowed a spectroscopic analysis of the Ru(IV)–cyanamide chromophore. Only $[(NH_3)_5Ru(Me_2dicyd)]^{2+}$ could be isolated with sufficient purity to permit NMR studies. While the ^{1}H-NMR spectrum is best characterized as being derived from a diamagnetic Ru(IV) complex, the *trans*-ammine protons are shifted downfield by 5.23 ppm relative to the *cis*-ammine protons [46]. This unusual anisotropy in chemical shifts was ascribed to a hyperconjugation interaction between the *trans*-ammine and the empty dπ orbital of Ru(IV),

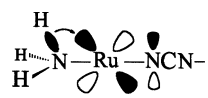

and is similar to the mechanism of solvent perturbation described above.

Substituting ammine ligands with pyridine moieties stabilizes the Ru(II) oxidation state and has allowed the isolation of the following Ru(II) complexes, *cis*-$[Ru(bpy)_2L_2]$ [47], *trans*-$[Ru(py)_4L_2]$ [48], Na[Ru(bmipy)(dcbpy)L] [49,50] and $[Ru(trpy)(bpy)L]^+$ [51] (py, pyridine; bpy, 2,2′-bipyridine; trpy, terpyridine; bmipy, 2,6-bis(1-methylbenzimidazol-2-yl)pyridine; and dcbpy, 4,4′-dicarboxylbipyridine) where L is a phenylcyanamide anion derivative. Crystal structures of *cis*-$[Ru(bpy)_2(4\text{-}NO_2pcyd)_2]$ [52], *trans*-$[Ru(py)_4(2\text{-}Clpcyd)_2]$ [48], and $[Ru(trpy)(bpy)(2,4\text{-}Clpcyd)]^+$ [51] all showed monodentate phenylcyanamido derivatives coordinated to Ru(II) through their cyano-nitrogens. These three complex families have been characterized by cyclic voltammetry and spectroelectrochemistry to explore the effect of inner-sphere perturbations on the Ru(III)–cyanamide chromophore. An ^{1}H-NMR study of the Na[Ru(bmipy)-(dcbpy)L] complexes showed evidence of linkage isomerism [49,50]. The initial isomer ratio of 1:1 changed to a ratio of 19:1 with prolonged reaction time. The authors suggested that the more stable cyano-bound isomer was preferred. In addition, the authors investigated these complexes for use as sensitizers in photovoltaic devices [51]. Overall solar energy conversion efficiencies were in the range of 3–4%. Unfortunately, a crystal structure determination was not performed from this family of complexes.

4.3.2. Dinuclear ruthenium complexes

4.3.2.1. Crystal structures. Crystal structures of the Ru(III) dinuclear complexes, $[\{(NH_3)_5Ru\}_2(\mu\text{-dicyd})]^{4+}$ [8], *trans*-,*trans*-$[\{(NH_3)_4Ru(py)\}_2(\mu\text{-dicyd})]^{4+}$, where py, pyridine [31]; and *mer*-,*mer*-$[\{(NH_3)_3Ru(bpy)\}_2(\mu\text{-dicyd})]^{4+}$, where bpy is 2,2′-bipyridine [32] have been performed. A representative ORTEP drawing of *mer*-,*mer*-$[\{(NH_3)_3Ru(bpy)\}_2(\mu\text{-dicyd})]^{4+}$ is shown in Fig. 6. The bond lengths and angles that make up the Ru(III) coordination sphere are similar to those of the mononuclear complexes (Section 4.3.1) but the bridging ligand deserves special mention. A characteristic of coordinated $dicyd^{2-}$ is that it retains its planarity upon coordination in the solid state. This has important consequences to electron exchange and is discussed in Section 4.3.2.2. The *anti* configuration of cyanamide groups, while observed in Fig. 6 and in the crystal structure of $[\{(NH_3)_5Ru\}_2(\mu\text{-dicyd})]^{4+}$, is not a constant. The crystal structure of *trans*-,*trans*-$[\{(NH_3)_4Ru(py)\}_2(\mu\text{-dicyd})]^{4+}$ showed a planar $dicyd^{2-}$ with cyanamide groups adopting a *syn* conformation [31]. This implies that in solution the cyanamide groups may rotate about the phenyl ring. The barrier for this rotation is likely to be small for the free ligand but for a dinuclear complex, resonance exchange between the metals should make a significant contribution to the rotation barrier. In addition, the crystal structure of $[\{(NH_3)_5Ru\}_2(\mu\text{-dicyd})]^{4+}$ [8], showed two Ru(III)–cyanamide conformations, the commonly observed linear coordination mode (Ru(III)–NCN bond angle of 175.1°) and a bent coordination mode (Ru(III)–NCN bond angle of 149.8°). There have been no crystal structure determinations performed on analogous Ru(II) or mixed-valence complexes.

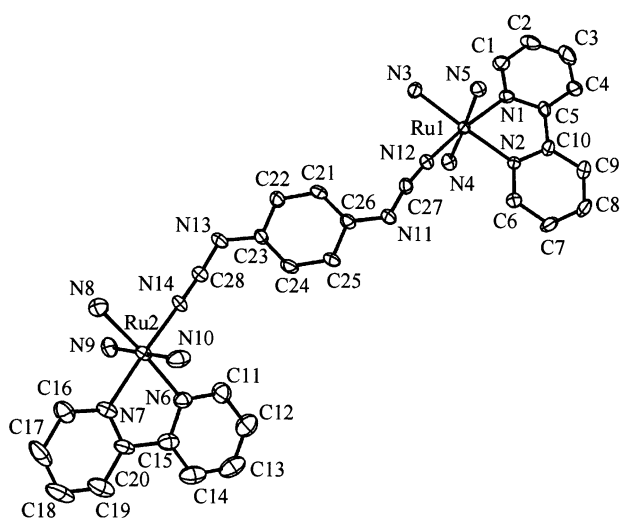

Fig. 6. ORTEP of the *mer*-,*mer*-$[\{Ru(NH_3)_3(bpy)\}_2(\mu\text{-dicyd})]^{4+}$ cation, from Ref. [32a] and reproduced with permission from the American Chemical Society.

4.3.2.2. Antiferromagnetic exchange. If two metal ions with spin $S = 1/2$ are antiferromagnetically coupled, a singlet ground state (^{1}S) and an excited triplet state (^{3}S) are created with a separation of energy equal to $-2J$, where J is the exchange coupling constant. J is negative in the case of antiferromagnetic exchange. This specific case is shown below

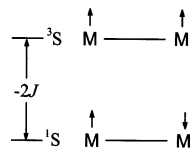

For many dinuclear systems, the distance between metal orbitals precludes direct overlap and yet antiferromagnetic exchange occurs because of the superexchange mechanism in which the orbitals of the bridging ligand directly participate in electron exchange through a LMCT transition

In the LMCT excited state, the unpaired electrons can couple but can do so only if their spins are opposite. The mixing of the LMCT excited state with the ground state therefore stabilizes a ground state in which the electrons are antiparallel. Optimization of superexchange requires that the ligand orbital (usually the highest occupied molecular orbital, HOMO) be energy and symmetry matched with the magnetic orbitals (orbitals containing one electron), and that its overlap with these orbitals be simultaneous.

For Ru(III) ions bridged by a planar dicyd^{2-}, the HOMO superexchange pathway possesses π symmetry, (Fig. 7), and the Ru(III) ions are predicted to be antiferromagnetic coupled despite a separation between Ru(III) ions of 13 Å. Extended Hückel calculations have shown that essentially the same electron density coefficients are seen for the bridging ligand HOMO (Fig. 7) if the cyanamide groups adopt a *syn* conformation. Importantly, temperature-dependent magnetic susceptibility measurements of the $[\{(NH_3)_5Ru\}_2(\mu\text{-L})]^{4+}$ complexes where L = Me_2dicyd^{2-}, dicyd^{2-}, Cl_2dicyd^{2-}, and Cl_4dicyd^{2-} all show antiferromagnetic exchange with the magnitude of $-J$ increasing with decreasing energy gap between

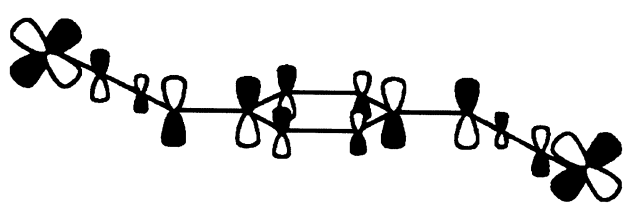

Fig. 7. The superexchange pathway in dinuclear ruthenium complexes bridged by dicyd^{2-}. For the bridging dicyd^{2-} ligand, the size of the p-orbital reflects its contribution to the HOMO, according to the extended Hückel calculation of the ligand.

Ru(III) and the HOMO of the bridging ligand [8]. The complex $[\{(NH_3)_5Ru\}_2(\mu\text{-}Me_4dicyd)]^{4+}$ does not follow this energy gap relationship and it has been suggested that the observed weak antiferromagnetic exchange is a consequence of the non-planarity of the bridging ligand [23]. The complexes *trans*-,*trans*-$[\{(NH_3)_4Ru(py)\}_2(\mu\text{-dicyd})]^{4+}$, and *mer*-,*mer*-$[\{(NH_3)_3Ru(bpy)\}_2(\mu\text{-dicyd})]^{4+}$, are diamagnetic in the solid state which indicates that $-J \geq 400\ cm^{-1}$ [31,32].

These complexes show a dramatic dependence of antiferromagnetic exchange upon the nature of the outer coordination sphere. A key to understanding this effect is the solvent dependence of the Ru(III)–cyanamide chromophore already discussed in Section 4.3.1.2. Fig. 8 shows the solvent dependence of the lowest energy LMCT band of $[\{(NH_3)_5Ru\}_2(\mu\text{-dicyd})]^{4+}$ [53]. The rapid decrease in LMCT band oscillator strength results from the decoupling of Ru(III) ions from the cyanamide groups because of the outersphere donor–acceptor interaction between the solvents's non-bonding electron pairs and the protons of the ammine ligands. If the Ru(III) ions are decoupled from the cyanamide groups, it follows that the Ru(III) ions are decoupled from the superexchange pathway and that antiferromagnetic exchange will be weakened. This will result in an increase in paramagnetism, which will have a dramatic effect on the complexes' ^{1}H-NMR spectra because of contact and pseudocontact shifts. This is illustrated by proton chemical shifts in Table 3 of $[\{(NH_3)_5Ru\}_2(\mu\text{-}Me_2dicyd)]^{4+}$ in a number of deuter-

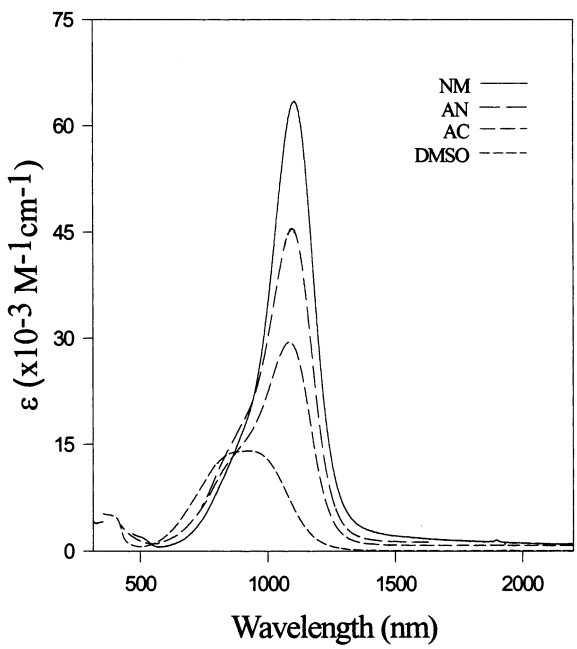

Fig. 8. Solvent dependence of the LMCT band of $[\{Ru(NH_3)_5\}_2(\mu\text{-dicyd})]^{4+}$ in nitromethane (NM), acetonitrile (AN), acetone (AC) and dimethylsulfoxide (DMSO), from Ref. [53] and reproduced with permission from the American Chemical Society.

Table 3
Solvent dependent ^{1}H-NMR chemical shifts of the complex, $[\{NH_3)_5Ru\}_2(\mu\text{-}Me_2dicyd)][PF_6]_4$

Deuterated solvents	Proton chemical shifts [a]			
	trans-NH_3	*cis*-NH_3	2,5-Methyl	3,6-Phenyl
Nitromethane	6.92	2.97	2.12	7.10
Acetonitrile	18.75	5.58	3.75	5.27
Acetone	36.87	10.49	5.91	2.91
DMSO	167.17	43.81	17.11	−8.44
Water	[b]	[b]	17.04	−6.58

[a] Bruker AMX-400 NMR spectrometer; all chemical shifts are singlets and gave the correct integration for their assignment. The values in ppm are referenced to TMS (0.00 ppm) for nonaqueous and to DSS (0.00 ppm) for D_2O, from Ref. [54].
[b] Not observed because of rapid deuterium exchange.

ated solvents [54]. While the chemical shifts of this complex in nitromethane are those that are expected for a diamagnetic complex, the chemical shifts in DMSO are wildly shifted and indicate significant paramagnetism.

By using the Evans method, it was possible to measure the room temperature magnetic moment of the $[\{(NH_3)_5Ru\}_2(\mu\text{-dicyd})]^{4+}$ family of complexes in nitromethane, acetonitrile, acetone, and DMSO [55] and from these values it is possible to calculate corresponding J values according to the method of Thompson and Ramaswamy [56]. By using valence-bond theory, antiferromagnetic exchange J_{AF} can be related to metal–ligand coupling elements according to [57]

$$-J_{AF} = \frac{h_{d\pi}^4}{\Delta^2}\left(\frac{1}{U} + \frac{2}{E_{DCT}}\right) \tag{3}$$

where the transfer integral (metal–ligand coupling element), $h_{d\pi}$, corresponds to a one-electron charge transfer between the bridging ligand and the metal (i.e. an LMCT transition), Δ the energy difference between the ground state and the LMCT excited state associated with $h_{d\pi}$, U the metal-to-metal charge transfer MMCT transition energy and E_{DCT} is the difference in energy between the ground and double charge transfer states. Creutz et al. have shown [4] that the value of $h_{d\pi}$ can be determined from experimental CT band properties by using the expression from Mulliken and Hush

$$h_{d\pi} = \frac{3.03 \times 10^2}{r}(\nu_{max} f)^{1/2} \tag{4}$$

where ν_{max} is the band maximum in cm^{-1}, f the oscillator strength of a single metal–ligand chromophore, and r the transition moment length which is usually taken to be the separation between donor and acceptor in Å.

The correlation between the theoretically derived J_{AF} and that derived from magnetic moments J_{est} (Fig. 9) is quite good for data derived from aprotic solvents but the difference between aprotic and protic data suggest that there are two pathways for antiferromagnetic superexchange [55].

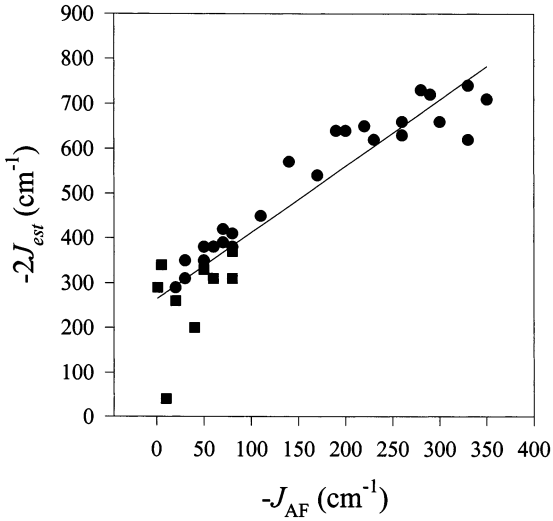

Fig. 9. Plot of calculated versus estimated antiferromagnetic exchange constants for the complexes in aprotic solvents (solid circles) and the complexes in aqueous solutions (solid squares), from Ref. [55] and reproduced with permission from the American Chemical Society. The equation for the line is $2J_{est} = 1.5J_{AF} - 260$, $R^2 = 0.86$.

4.3.2.3. Mixed-valence complexes. The stability of a mixed-valence complex relative to its oxidized and reduced forms is defined by the comproportionation equilibrium Eq. (5)

$$[III,III] + [II,II] \overset{K_c}{\rightleftharpoons} 2[III,II] \tag{5}$$

which for ruthenium dinuclear complexes can be calculated from the difference between Ru(III/II) couples (ΔE in V) according to

$$K_c = 10^{16.91\Delta E} \tag{6}$$

The magnitude of K_c is determined by the sum of all energetic factors relating to the stability of the reactant and the product complexes according to the equation [53] for the free energy of comproportionation, ΔG_c:

$$\Delta G_c = \Delta G_s + \Delta G_e + \Delta G_i + \Delta G_r + \Delta G_{ex} \tag{7}$$

In Eq. (7), ΔG_s reflects the statistical distribution of the comproportionation equilibrium, ΔG_e accounts for the electrostatic repulsion of the two like-charged metal centers, ΔG_i is an inductive factor dealing with competitive coordination of the bridging ligand by the metal ions, ΔG_r is the free energy of resonance exchange; the only component of ΔG_c which represents "actual" metal–metal coupling and finally ΔG_{ex}, is the term to account for the antiferromagnetic exchange stabilization of [III,III] in Eq. (5).

The electronic properties of mixed-valence complexes are understood within the framework of Marcus–Hush theory as illustrated by the potential energy diagrams

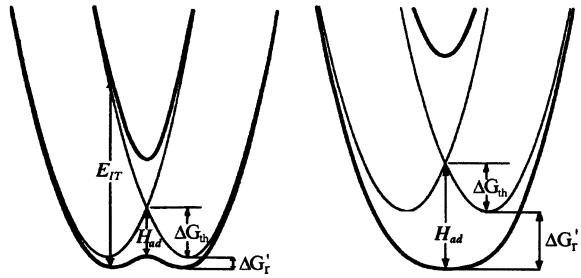

Fig. 10. Potential energy curves for Class I (light line in both A and B), Class II (A) and Class III (B) symmetric mixed-valence complexes, from Ref. [53] and reproduced with permission from the American Chemical Society.

in Fig. 10. Mixed-valence complexes are classified according to the degree of metal–metal coupling [58]. For a Class I complex, metal ions are electronically isolated and the properties of the complex are much the same as that observed for similar mononuclear complexes. For a Class II complex, metal ions are coupled but there is still a thermal barrier to electron transfer between the metal ions and so the metal ions possess different oxidation states. For a Class III complex, metal–metal coupling is of sufficient magnitude to eliminate the thermal barrier to electron transfer. The odd electron is delocalized between the two metal ions, which possess equivalent fractional oxidation states.

The mechanism of metal–metal coupling in mixed-valence complexes usually involves either electron transfer (LUMO pathway) or hole transfer (HOMO pathway) superexchange. For a π-donor aromatic system such as the $dicyd^{2-}$ bridging ligand, hole transfer superexchange is the dominant mechanism for metal–metal coupling and so the energy gap between metal acceptor orbital and the HOMO of the bridging ligand is a critical factor. As has already been discussed in Section 4.3.2.2, this energy gap can be "tuned" by changing the nature of the auxiliary ligands or by the substituents on the phenyl ring of the bridging ligand. Towards this end, the following families of ruthenium mixed-valence complexes were studied, $[\{(NH_3)_5Ru\}_2(\mu\text{-dicyd})]^{3+}$ [8], *trans*-,*trans*-$[\{(NH_3)_4Ru(py)\}_2(\mu\text{-dicyd})]^{3+}$ [31], and *mer*-,*mer*-$[\{(NH_3)_3Ru(bpy)\}_2(\mu\text{-dicyd})]^{3+}$ [32], $[\{Ru(bpy)(trpy)\}_2(\mu\text{-dicyd})]^{3+}$ [26], and $[\{(NH_3)_5Ru\}_2(\mu\text{-bp})]^{3+}$ (bp, 4,4′-dicyanamidobiphenyl) [11].

$[\{(NH_3)_5Ru\}_2(\mu\text{-bp})]^{3+}$ is a very weak Class II complex whose intervalence spectral data required a correction for the comproportionation equilibrium Eq. (5). The complex's weak metal–metal coupling compared to its $dicyd^{2-}$ analogue was rationalized by the greater stability of the HOMO of bp^{2-}, which is 780 mV more positive than the HOMO of $dicyd^{2-}$ [11]. $[\{Ru(bpy)(trpy)\}_2(\mu\text{-dicyd})]^{3+}$ appeared to be a Class III system whose comproportionation equilibrium showed a significant effect from the free energy of antiferromagnetic exchange [26,32]. The effect of changing the energy of the bridging ligand HOMO was explored by the study of the

mixed-valence complexes *trans*-,*trans*-$[\{(NH_3)_4Ru(py)\}_2(\mu\text{-}L)]^{3+}$ ($L = Cl_4dicyd^{2-}$, Cl_2dicyd^{2-}, $dicyd^{2-}$, Me_2dicyd^{2-}) [31]. For strongly coupled Class II systems, ΔG_c is largely determined by the free energy of resonance exchange ΔG_r which in turn is determined by the magnitude of metal–metal coupling. Thus the observed increase in ΔG_c with decreasing energy gap between metal and bridging ligand is entirely consistent with the hole-transfer superexchange mechanism [31]. The effect of replacing ammine ligands with pyridine moieties in these complexes was also examined [32]. Because ammine ligands are strong donors, replacing them with pyridine moieties stabilizes the ruthenium dπ orbitals and reduces the energy gap for superexchange. As shown in Fig. 11, which plots the number of ammine ligands in a dinuclear ruthenium complex against ΔG_c and intervalence band oscillator strength, the correlation is not linear. In particular, the leveling of ΔG_c for the Class III complex $[\{Ru(bpy)(trpy)\}_2(\mu\text{-dicyd})]^{3+}$ was ascribed to a large contribution from ΔG_{ex} (Eq. (7)) [32].

The magnitude of metal–metal coupling in the above polyammineruthenium mixed-valence complexes can be dramatically perturbed by the nature of solvent [53,54,59]. Fig. 12 shows the cyclic voltammogram of $[\{(NH_3)_5Ru\}_2(\mu\text{-dicyd})]^{4+}$ in water and acetonitrile. In water two waves at positive potential (> 0.4 V) are single electron ligand oxidation waves. The large wave centered at 0.05 V, represents two Ru(III/II) couples superimposed because of very weak metal–metal coupling. In acetonitrile, these two waves split apart because of dramatically increased metal–metal coupling. The origin of this effect is the donor–acceptor interaction between the ammine protons and the solvent lone pairs already discussed in Sections 4.3.1 and 4.3.2.2. Thus, by changing the donor properties of the solvent one can perturb superexchange within the Ru^{II}–dicyd–Ru^{III} system. In conjunction with inner-

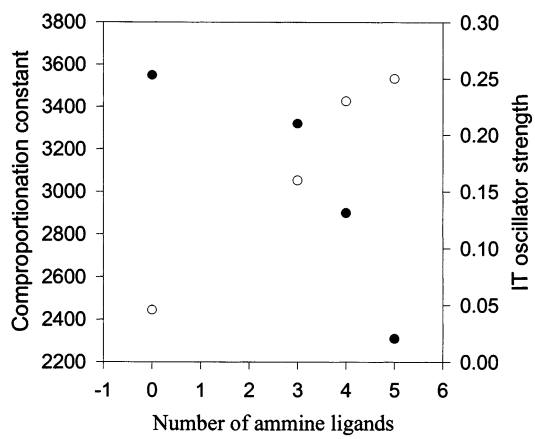

Fig. 11. Plot showing the effect of replacing ammine ligands with pyridine moieties on the free energy of comproportionation (●) and the IT oscillator strength (○) of ruthenium dinuclear complexes in acetonitrile, $[\{Ru(NH_3)_5\}_2(\mu\text{-dicyd})]^{3+}$ for $n = 5$, *trans*-,*trans*-$[\{Ru(NH_3)_4(pyridine)\}_2(\mu\text{-dicyd})]^{3+}$ for $n = 4$, *mer*-,*mer*-$[\{Ru(NH_3)_3(bpy)\}_2(\mu\text{-dicyd})]^{3+}$ for $n = 3$ and $[\{Ru(terpy)(bpy)\}_2(\mu\text{-dicyd})]^{3+}$ for $n = 0$, from Ref. [32a] and reproduced with permission from the American Chemical Society.

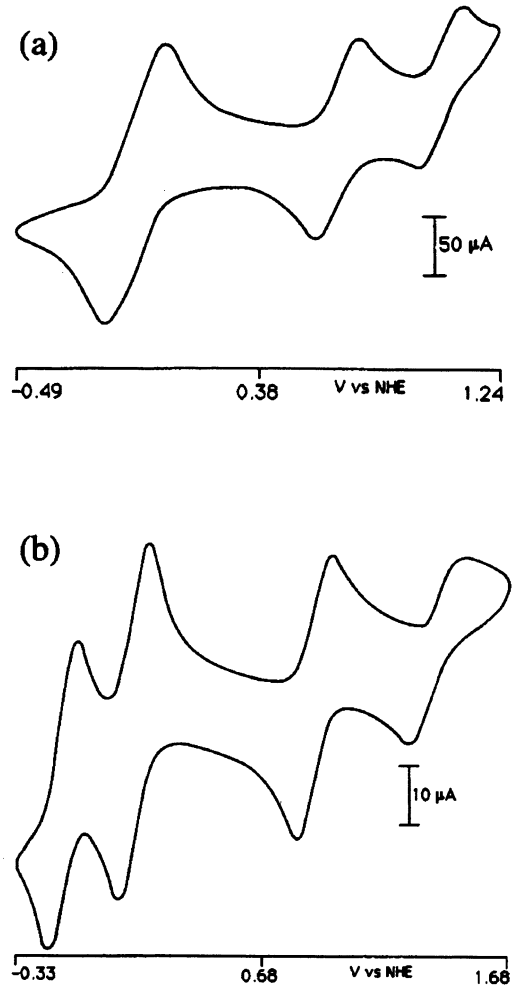

Fig. 12. Cyclic voltammetry of $[\{Ru(NH_3)_5\}_2(\mu\text{-dicyd})][PF_6]_4$ in: (a) aqueous; and (b) acetonitrile solutions, from Ref. [59].

sphere modifications that were discussed above, this creates a wealth of mixed-valence complex data that should be amendable to theory.

Creutz et al. recently developed a model for metal–metal coupling elements [4]

$$H_{MM'} = \frac{H_{ML}H_{M'L}}{2\Delta E^{eff}_{ML}} + \frac{H_{LM}H_{LM'}}{\Delta E^{eff}_{LM}} \quad (8)$$

The coupling element $H_{MM'}$ of Eq. (8) is the effective metal–metal coupling, while the coupling elements in the two terms on the right of Eq. (8) are associated with metal–ligand interactions of the electron-transfer and hole-transfer pathways, respectively, which can be calculated from the appropriate charge transfer spectral

data and Eq. (4). The denominators are reduced energy gaps between metal and ligand orbitals. The subscript nomenclature may be understood given that the electron-transfer pathway is associated with metal-to-ligand charge transfer (MLCT) bands in the electronic spectrum of the complex, while the hole-transfer pathway is associated with ligand-to-metal (LMCT) bands. For the case of a dominating hole-transfer superexchange pathway, Eq. (8) can be simplified to [53]

$$H_{MM'} = \frac{H_{LM}^2}{\Delta E_{LM}^{eff}} \tag{9}$$

Recognizing that for a Class II system [60]

$$\Delta G_r' = \frac{H^2}{E_{IT}} \tag{10}$$

it is possible to compare the $\Delta G_r'$ values derived from spectroscopy and theory to experimental values derived from cyclic voltammetry. The result of this comparison in Fig. 13 shows an excellent correlation of experiment to theory and strongly support the relationship between metal–ligand and metal–metal coupling elements to charge-transfer band oscillator strengths described by Eq. (8) [53].

There is a single example of a [IV,III] complex, $[\{Ru(NH_3)_5\}_2(\mu\text{-}Me_2dicyd)]^{5+}$ which was studied by UV–vis and ^{1}H-NMR spectroscopy. The simplicity of the ^{1}H-NMR spectrum suggested that the ruthenium ions were equivalent on the NMR time scale [46].

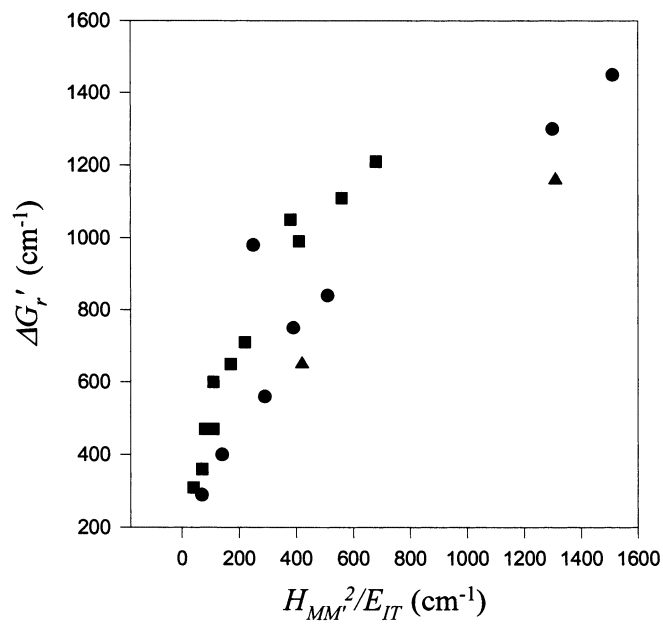

Fig. 13. Plot of $\Delta G_r'$ versus $H_{MM'}^2/E_{IT}$ for the pentaammine (■), tetraammine (●) and triammine (▲) complexes. The data may be found in Ref. [53] and the figure is reproduced with permission from the American Chemical Society.

4.4. Cobalt complexes

The complexes, $[Ph_4As]_2[CoL_4]$, where L = pcyd$^-$, 3,5-Cl_2pcyd$^-$, 2,4-F_2pcyd$^-$, 2,4,6-Cl_3pcyd$^-$, 2-Clpcyd$^-$, and 2,4,6-Me_3pcyd$^-$, were prepared by reacting four equivalents of a Ag(I) or Tl(I) phenylcyanamide salt with tetraphenylarsonium tetrachlorocobaltate in dry degassed dichloromethane. [5]. $[Ph_4As]_2$[Co(2,4,6-Me_3pcyd)$_4$] proved unstable as a solid and did not give acceptable elemental analysis.

4.5. Nickel, palladium and platinum complexes

Salts of $[NiL_4]^{2-}$ where L = 2-Clpcyd^{2-} and 2,4,6-Cl_3pcyd$^-$, were prepared in order to compare the ligand field properties of phenylcyanamide ligands to other pseudo-halogens [5]. These phenylcyanamide ligands appeared to be stronger field ligands than the halides but weaker than NCO^- or NCS^- ions. The ligand field spectral data are consistent with tetrahedral or distorted tetrahedral Ni(II) coordination sphere geometry.

The complex family [Ni(imd)L] where imd, 1,3-bis-(2-pyridylimino)isoindolinato and L = 2-Clpcyd$^-$, 4-Clpcyd$^-$, 2,3-Cl_2pcyd$^-$, 2,6-Cl_2pcyd$^-$, 2,4,5-Cl_3pcyd$^-$, 2,3,5,6-Cl_4pcyd$^-$, were characterized by IR, ^{1}H-NMR, and UV–vis spectroscopy [61]. The crystal structure of [Ni(imd)(2-Clpcyd)] shows Ni(II) in a distorted square planar coordination sphere of nitrogen donor atoms in which the phenylcyanamide ligand is coordinated to Ni(II) through the cyano-nitrogen. The complex is not planar as the phenyl ring of the phenylcyanamide ligand is perpendicular to the Ni(II) square planar coordination sphere.

Palladium and platinum complexes have been synthesized with the chemical formula [M(trpy)L][PF_6], M = Pd(II) and Pt(II) and L = pcyd$^-$, 2-Clpcyd$^-$, 2,3-Cl_2pcyd$^-$, 2,6-Cl_2pcyd$^-$, 2,4,6-Cl_3pcyd$^-$, 2,3,4,5-Cl_4pcyd$^-$ and Cl_5pcyd$^-$ [62,63]. These complexes were characterized by ^{1}H-NMR and electronic absorption spectroscopy and cyclic voltammetry. Fig. 14 shows the crystal structure of [Pd(trpy)(2,6-Cl_2pcyd)][PF_6] [62]. Importantly, the complex cation is approximately planar with a dihedral angle of 2.16(16)° between the best fit of the palladium coordination sphere and that for the phenyl ring of the phenylcyanamide ligand. Dimerization in the solid state is suggested by the distance of 3.265 Å between Pd(II) and the amide nitrogen from the neighboring complex, (Section 4.1, bridging mode I), which is significantly closer than van der Waals contact.

Organic charge-transfer salts can be highly conducting and a characteristic feature in the crystal lattice of these materials is the orientation of conjugated planar molecules on top of one another to form ''pancake'' stack structures. Under the right conditions, the π interactions between the molecules in the stacks result in conductivity in the direction of the π stacks [64]. With this in mind and the knowledge that $[M(trpy)L]^+$ cations are planar, the dinuclear complexes [{Pt(trpy)}$_2$(μ-L)][PF_6]$_2$, L = dicyd^{2-}, Cl_2dicyd^{2-} and Me_2dicyd^{2-}, have been synthesized [63]. Unfortunately, the complexes were not amenable to crystallization to confirm the presence of π stacking. Nevertheless, preliminary results of I_2 doping of

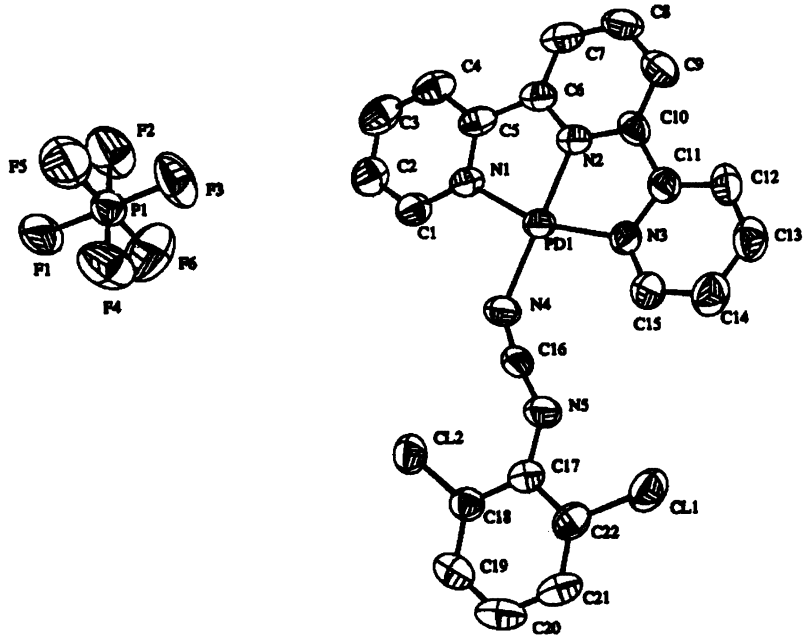

Fig. 14. ORTEP diagram of the complex [Pd(trpy)(2,6-Cl_2pcyd)][PF_6] from Ref. [62] and reproduced with permission from the American Chemical Society.

[{Pt(trpy)}$_2$(μ-Me_2dicyd)][PF_6]$_2$, did show powder conductivity consistent with semiconductor properties [16].

4.6. Copper and silver complexes

The first crystal structure of a transition metal complex of a phenylcyanamide anion ligand was [{Cu(bpy)(pcyd)}$_2$(μ-pcyd)$_2$] (Fig. 15) and showed both monodentate phenylcyanamide (cyano-nitrogen) and bridging phenylcyanamide (mode I) coordination with Cu(II) in a distorted square pyramidal coordination sphere [65,66]. In contrast, a crystal structure of the complex [Cu(bpy)(2,3-Cl_2pcyd)$_2$] showed only monodentate phenylcyanamide ligands coordinated through the cyano-nitrogen and Cu(II) in a distorted square plane of nitrogen donor atoms [33]. It was suggested that the reason dimerization does not occur for this complex, may be the greater steric crowding of the chlorine atoms and/or the inductive effect of chlorine which makes the cyanamide group less basic and therefore a poorer bridging ligand. Other Cu(II) complexes [66] possessing the formula [Cu(bpy)L_2], L = 4-Clpcyd$^-$, 3-Clpcyd$^-$, 2-Clpcyd$^-$, 4-Brpcyd$^-$, 4-Fpycd$^-$, 4-Mepcyd$^-$, 2-Mepcyd$^-$, 4-MeOpcyd$^-$, and the analogous phenanthroline complexes, [Cu(phen)L_2], may be dinuclear in the solid state. The complexes [Cu(pip)$_2L_2$], where pip, piperidine; L = pcyd$^-$, 4-Clpcyd$^-$, and 4-Brpcyd$^-$, [Cu(py)$_4L_2$], where L = pcyd$^-$, 4-Clpcyd$^-$, 3-Clpcyd$^-$, 4-Brpcyd$^-$, and 4-Fpcyd$^-$, [{Cu(bpy)(2-Mep-

cyd)$(CH_3CO_2)\}_2$], and [$\{$Cu(phen)(L)$(CH_3CO_2)\}_2$], where L = 3-Clpcyd$^-$ and 3-MeOpcyd$^-$ have been synthesized [66]. All the above Cu(II) complexes were characterized by IR and UV–vis spectroscopy. The magnetic moments of these complexes lie in the range of 1.8–2.1 BM close to the spin only value for Cu(II) ions. In particular, the magnetic moment of [$\{$Cu(phen)(3-Clpcyd)$(CH_3CO_2)\}_2$] (1.89 BM/Cu(II)) is rather surprising given that the copper ions are bridged by only a single nitrogen atom as shown by its crystal structure in Fig. 16. The bridging does involve orthogonal Cu(II) d-orbitals and so perhaps low-temperature studies might reveal ferromagnetic coupling. Fig. 16 shows the first example of a phenylcyanamide ligand adopting bridging mode II.

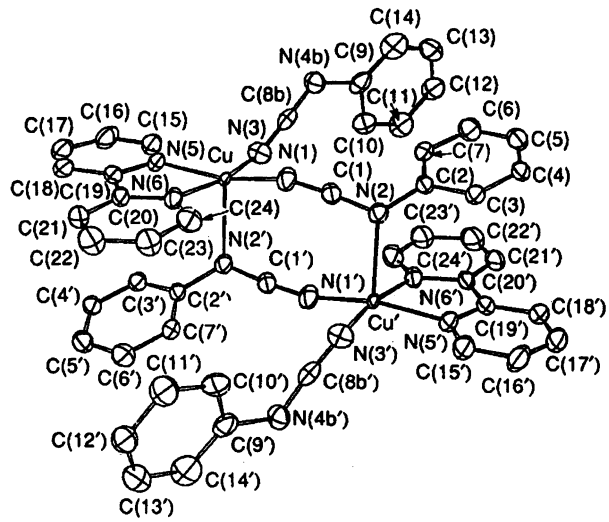

Fig. 15. ORTEP of the complex, [$\{$Cu(bpy)(pcyd)$\}_2$(μ-pcyd)$_2\}$] from Ref. [66] and reproduced with permission from The Royal Society of Chemistry.

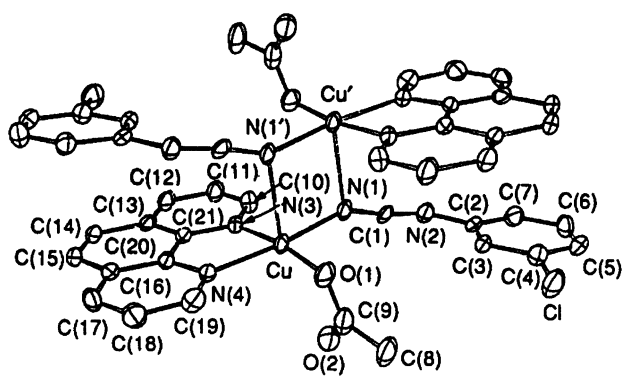

Fig. 16. ORTEP of the complex [$\{$Cu(phen)$(CH_3CO_2)\}_2$(μ-3-Clpcyd)$_2$], from Ref. [66] and reproduced with permission from The Royal Society of Chemistry.

The $[Cu(bpy)_2L][PF_6]$ complexes, where L = 2-Clpcyd$^-$, 4-Clpcyd$^-$, 2,3-Cl_2pcyd$^-$, 2,6-Cl_2pcyd$^-$, 2,4,5-Cl_3pcyd$^-$, and 2,3,5,6-Cl_4pcyd$^-$, were synthesized by reacting the thallium phenylcyanamide salt with $[Cu(bpy)_2Br][PF_6]$ in acetonitrile [33]. These complexes were characterized by electronic absorption, IR spectroscopy and cyclic voltammetry. A crystal structure of $[Cu(bpy)_2(2,3\text{-}Cl_2pcyd)][PF_6]$ showed copper in a distorted square pyramid of nitrogen donor atoms in which the cyanamido ligand coordinates via its cyano-nitrogen to an equatorial site. In addition to d–d transitions that were centered around 700 nm, the complexes possess an additional band ca. 500 nm that is assigned to a $\pi \rightarrow \sigma^*$ LMCT transition of the Cu(II)–NCN chromophore. When the LMCT energy of the $[Cu(bpy)_2L]^+$ complexes is plotted against the LMCT energy of the $[Ru(NH_3)_5L]^{2+}$ complexes, a positive linear correlation is obtained which supports the validity of this assignment.

Cu(I) complexes possessing the formulae $[Cu_2(dppe)_3L_2] \cdot 2(CH_3)_2CO$, (dppe, 1,2-bis(diphenylphosphino)ethane, L = pcyd$^-$, 4-Clpcyd$^-$, 3-Clpcyd$^-$, 4-Brpycd$^-$, and 4-Fpcyd$^-$) and $[\{Cu(PPh_3)_2L\}_2]$, (L = pcyd$^-$, 4-Clpcyd$^-$, 3-Clpcyd$^-$, 4-Br-pycd$^-$, 4-Fpcyd$^-$, 4-Mepcyd$^-$, 4-MeOpcyd$^-$, 4-NO_2pcyd$^-$ and 4-Me_2Npcyd$^-$) were characterized by IR and ^{31}P-NMR spectroscopy and crystallography [34,67]. For the complex, $[\{Cu(PPh_3)_2\}_2(\mu\text{-}4\text{-}Mepcyd)_2]$, the cyanamide ligands coordinate to the Cu(I) ions according to bridging mode I (Section 4.1). A crystal structure of $[Cu_2(dppe)_3(4\text{-}Clpcyd)_2]$ was also performed and, in this case, the monodentate phenylcyanamide ligands coordinate via their cyano-nitrogen. In both structures, the Cu(I) ion occupies a distorted tetrahedral coordination sphere and the phenylcyanamide ligands are characteristically planar.

Solid state ^{31}P-cross polarization magic angle spinning NMR data have been obtained on three solid Cu(I) complexes $[\{Cu(PPh_3)_2\}_2(\mu\text{-}L)_2]$, where L = pcyd$^-$, 4-Mepcyd$^-$ and 4-Clpcyd$^-$, in varying magnetic fields [68]. Examination of the highly structured complex spectra showed that the asymmetry induced in the *J*-split multiplets from quadrupole effects in the P_2CuN_2 system is much smaller than is usually encountered in P_2CuX_2 (X = halogen) and P_2CuO_2 systems. It was suggested that this could be attributed to an unusually small electric field gradient at the copper site despite marked deviation of the copper coordination sphere from tetrahedral symmetry.

It is possible to form the mononuclear copper complexes $[Cu(PPh_3)_3L]$ (L = 4-NO_2pcyd$^-$ and 4-Me_2Npcyd$^-$) [67]. These were characterized by melting point, conductivity and IR spectroscopy. Attempts to grow crystals of these complexes resulted in contamination of the product with the dimeric complexes, $[\{Cu(PPh_3)_2\}_2(\mu\text{-}L)_2]$.

Salts of $[CuL_4]^{2-}$ where L = 2-Clpcyd$^-$ and 2,4,6-Cl_3pcyd$^-$, have been prepared and their ligand field spectra and magnetic moments were consistent with tetrahedral geometry [5].

A series of dinuclear Cu(II) complexes with the formulae $[\{Cu(dien)\}_2(\mu\text{-}L)][CF_3SO_3]_2$, where dien, diethylenetriamine, and $[\{Cu(imd)\}_2(\mu\text{-}L)]$ where L =

$dicyd^{2-}$, Cl_2dicyd^{2-}, and Me_2dicyd^{2-}, were prepared and characterized by IR, UV–vis and EPR spectroscopy and magnetic studies [69]. Evidence for intramolecular antiferromagnetic exchange was observed but this was significantly weaker than that observed for dinuclear Ru(III) complexes incorporating the $dicyd^{2-}$ bridging ligands (Section 4.3.2.2). It was suggested that the weak antiferromagnetic exchanged resulted from a symmetry and energy mismatch between Cu(II) σ^* magnetic orbitals and the π_{nb} orbitals of the bridging $dicyd^{2-}$ ligand which are important for superexchange.

Triphenylphosphinephenylcyanamidosilver(I) complexes, $[\{Ag(PPh_3)_2\}_2(\mu\text{-}4\text{-}Me_2Npcyd)_2]$ and $[Ag(PPh_3)_3L]$, where L = $pcyd^-$, 2-$Clpcyd^-$, 4-$Brpcyd^-$, 4-$MeOpcyd^-$, 4-NO_2pcyd^- or 4-Me_2Npcyd^-, were prepared and characterized by melting point, conductivity and IR spectroscopy and compared to their Cu(II) analogues [67]. Crystal structures of the dinuclear complexes $[\{M(PPh_3)_2\}_2(\mu\text{-}4\text{-}Me_2Npcyd)_2]$ (M = Cu(I) and Ag(I)) showed that the bridging cyanamide ligands adopted coordination mode I. In the case of the copper complex, the Cu(I) ions are centrosymmetric but for the silver complex the metal atoms are not equivalent. Crystal structures of the mononuclear complexes $[Ag(PPh_3)_3(4\text{-}Brpcyd)]$ and $[Ag(PPh_3)_3(4\text{-}MeOpcyd)]$ showed that the phenylcyanamide coordinates to Ag(I) through its terminal cyano-nitrogen and that Ag(I) is occupies a distorted tetrahedral coordination sphere.

5. Future studies

The coordination chemistry of phenylcyanamide ligands still requires much effort to complete. There are no examples of complexes of the early transition metals and of the middle and late transition metals, complexes of Fe, Os, Rh, Ir, Au and the Zn group are unknown. Neutral phenylcyanamide ligands should stabilize low-valent metals and may provide some unusual organometallic complexes. In this regard, the acidity of the amine proton and the possibility of side-on cyanamide group coordination may lead to some interesting chemistry. The ability of the $dicyd^{2-}$ bridging ligands to mediate metal–metal coupling suggests that phenylcyanamide derivatives may find their way into molecular materials possessing useful electronic and/or magnetic properties. In preliminary studies, copper(II) complexes of the 1,3-dicyanamidobenzene bridging ligand have been shown to form linear chains. These novel materials possess magnetic properties consistent with spin canting and so should contribute to our understanding of the origin of this effect.

Acknowledgements

The financial support of the Natural Sciences and Engineering Research Council of Canada is gratefully recognized.

References

[1] (a) R. Cortés, L. Lezama, F.A. Mautner, T. Rojo, in: M.M. Turnbull, T. Sugimoto, L.K. Thompson (Eds.), Molecular Based Magnetic Materials, Series 644, American Chemical Society, Washington, 1996, p. 187. (b) A.M. Golub, H. Köhler, V.V. Skopenko, Chemistry of the Pseudohalides, Elsevier, New York, 1986.

[2] (a) M. Kabešová, R. Boca, M. Melník, D. Valigura, M. Dunaj-Jurco, Coord. Chem. Rev. 140 (1995) 115. (b) R.A. Bailey, S.L. Kozak, T.W. Michelsen, W.N. Mills, Coord. Chem. Rev. 6 (1971) 407.

[3] (a) N.S. Hush, Prog. Inorg. Chem. 8 (1967) 357. (b) R.A. Marcus, J. Chem. Phys. 26 (1957) 867 and 872.

[4] C. Creutz, M.D. Newton, N. Sutin, Photochem. Photobiol. A: Chem. 82 (1994) 47.

[5] (a) B.R. Hollebone, R.S. Nyholm, J. Chem. Soc. A (1971) 332. (b) B.R. Hollebone, J. Chem. Soc. A (1971) 481. (c) B.R. Hollebone, M.J. Stillman, Inorg. Chim. Acta 42 (1980) 169.

[6] R.J. Crutchley, M.L. Naklicki, Inorg. Chem. 28 (1989) 1955.

[7] M.L. Naklicki, R.J. Crutchley, Inorg. Chem. 28 (1989) 4226.

[8] (a) M.A.S. Aquino, PhD thesis, Carleton University, 1991. (b) M.A.S. Aquino, F.L. Lee, E.J. Gabe, C. Bensimon, J.E. Greedan, R.J. Crutchley, J. Am. Chem. Soc. 114 (1992) 5130.

[9] M.L. Naklicki, PhD thesis, Carleton University, 1995.

[10] C.A. White, PhD thesis, Carleton University, 1999.

[11] M.A.S. Aquino, C.A. White, C. Bensimon, J.E. Greedan, R.J. Crutchley, Can. J. Chem. 74 (1996) 2201.

[12] E. Kühle, Angew. Chem. Int. Ed. Engl. 8 (1969) 20.

[13] A. Aumüller, S. Hünig, Liebigs Ann. Chem. (1986) 142.

[14] Y. Wu, D.C. Limburg, D.E. Wilkinson, G.S. Hamilton, Org. Lett. 2 (2000) 795.

[15] D.R. Armstrong, F.A. Banbury, I. Cragg-Hine, M.G. Davidson, F.S. Mair, E. Pohl, P.R. Raithby, R. Snaith, Angew. Chem. Int. Ed. Engl. 32 (1993) 1769.

[16] R.J. Crutchley, unpublished results.

[17] M.A.S. Aquino, R.J. Crutchley, F.L. Lee, E.J. Gabe, C. Bensimon, Acta Crystallogr. C 39 (1993) 1543.

[18] H.D. Schadler, M. Reimer, W. Schroth, Z. Chem. 24 (1984) 407.

[19] G.W. Buchanan, R.J. Crutchley, Magn. Reson. Chem. 32 (1994) 552.

[20] S.T. King, J.H. Strope, J. Chem. Phys. 54 (1971) 1289.

[21] C.E.B. Evans, D. Ducharme, M.L. Naklicki, R.J. Crutchley, Inorg. Chem. 34 (1995) 1350.

[22] M.A.S. Aquino, A.E. Bostock, R.J. Crutchley, Inorg. Chem. 29 (1990) 3641.

[23] M.A.S. Aquino, F.L. Lee, E.J. Gabe, J.E. Greedan, R.J. Crutchley, Inorg. Chem. 30 (1991) 3234.

[24] C.K. Mann, K.K. Barnes, Electrochemical Reactions in Nonaqueous Systems, Marcel Dekker, New York, 1970.

[25] A. Aumüller, S. Hünig, Liebigs Ann. Chem. (1986) 165.

[26] A.R. Rezvani, C.E.B. Evans, R.J. Crutchley, Inorg. Chem. 34 (1995) 4600.

[27] R. Kato, H. Kobayashi, A. Kobayashi, J. Am. Chem. Soc. 111 (1989) 5224 (and references therein).

[28] A. Aumüller, P. Erk, G. Klebe, S. Hünig, U. Von Schutz, H.-P. Werner, Angew. Chem. Int. Ed. Engl. 25 (1986) 740.

[29] M.H. Chisholm, K. Folting, J.C. Huffman, N.S. Marchant, Polyhedron 3 (1984) 1033.

[30] R.J. Crutchley, K. McCaw, F.L. Lee, E.J. Gabe, Inorg. Chem. 29 (1990) 2576.

[31] (a) A.R. Rezvani, C. Bensimon, B. Cromp, C. Reber, J.E. Greedan, V.V. Kondratiev, R.J. Crutchley, Inorg. Chem. 36 (1997) 3322. (b) A.R. Rezvani, PhD thesis, Carleton University, 1995.

[32] (a) C.E.B. Evans, G.P.A. Yap, R.J. Crutchley, Inorg. Chem. 37 (1998) 6167. (b) C.E.B. Evans, PhD thesis, Carleton University, 1997.

[33] R.J. Crutchley, R. Hynes, E.J. Gabe, Inorg. Chem. 29 (1990) 4921.

[34] E.W. Ainscough, E.N. Baker, M.L. Brader, A.M. Brodie, S.L. Ingham, J.M. Waters, J.V. Hanna, P.C. Healy, J. Chem. Soc. Dalton Trans. (1991) 1243.

[35] R.E. Clarke, P.C. Ford, Inorg. Chem. 9 (1970) 227.

[36] R.D. Foust, P.C. Ford, Inorg. Chem. 11 (1972) 899.
[37] R.R. Gagné, C.A. Korval, G.C. Lisensky, Inorg. Chem. 19 (1980) 2855.
[38] T. Gennett, D.F. Milner, M.J. Weaver, J. Phys. Chem. 89 (1985) 2787.
[39] T.J. Meyer, Prog. Inorg. Chem. 30 (1983) 389.
[40] A.B.P. Lever, Inorganic Electronic Spectroscopy, 2nd ed., Elsevier, New York, 1984.
[41] A.A. Saleh, R.J. Crutchley, Inorg. Chem. 29 (1990) 2132.
[42] R.S. Mulliken, J. Chem. Phys. 7 (1939) 14 (see also p. 20).
[43] R.S. Mulliken, C.A. Reike, Rep. Prog. Phys. 8 (1941) 231.
[44] R.J. Crutchley, A.A. Saleh, K. McCaw, M.A.S. Aquino, Mol. Cryst. Liq. Cryst. 194 (1991) 93.
[45] S.K. Doorn, J.T. Hupp, J. Am. Chem. Soc. 111 (1989) 4704.
[46] M.L. Naklicki, C.A. White, V.V. Kondratiev, R.J. Crutchley, Inorg. Chim. Acta 242 (1996) 63.
[47] A.R. Rezvani, R.J. Crutchley, Inorg. Chem. 33 (1994) 170.
[48] P. Desjardins, G.P.A. Yap, R.J. Crutchley, Inorg. Chem. 38 (1999) 5901.
[49] S. Ruile, O. Kohle, P. Pechy, M. Gratzel, Inorg. Chim. Acta 261 (1997) 129.
[50] S. Ruile, O. Kohle, H. Pettersson, M. Gratzel, New J. Chem. 22 (1998) 25.
[51] P. Mosher, G.P.A. Yap, R.J. Crutchley, submitted for publication.
[52] P. Desjardins, MSc thesis, Carleton University, 1998.
[53] C.E.B. Evans, M.L. Naklicki, A.R. Rezvani, C.A. White, V.V. Kondratiev, R.J. Crutchley, J. Am. Chem. Soc. 120 (1998) 13 096.
[54] M.L. Naklicki, R.J. Crutchley, J. Am. Chem. Soc. 116 (1994) 6045.
[55] M.L. Naklicki, C.A. White, L.L. Plante, C.E.B. Evans, R.J. Crutchley, Inorg. Chem. 37 (1998) 1880.
[56] L.K. Thompson, B.S. Ramaswamy, Inorg. Chem. 25 (1986) 2664.
[57] F. Tuczek, E.I. Solomon, Inorg. Chem. 32 (1993) 2850.
[58] M.B. Robin, P. Day, Adv. Inorg. Chem. Radiochem. 10 (1967) 247.
[59] M.L. Naklicki, R.J. Crutchley, Inorg. Chim. Acta 225 (1994) 123.
[60] B.S. Brunschwig, N. Sutin, Coord. Chem. Rev. 187 (1999) 233.
[61] R.J. Letcher, W. Zhang, C. Bensimon, R.J. Crutchley, Inorg. Chim. Acta 210 (1993) 183.
[62] (a) W. Zhang, C. Bensimon, R.J. Crutchley, Inorg. Chem. 32 (1993) 5808. (b) W. Zhang, MSc thesis, Carleton University, 1993.
[63] F. Al-Mutlaq, MSc thesis, Carleton University, 1999.
[64] J.R. Ferraro, J.M. Williams, Introduction to Synthetic Electrical Conductors, Academic Press, New York, 1987.
[65] M.L. Brader, E.W. Ainscough, E.N. Baker, A.M. Brodie, Polyhedron 8 (1989) 2219.
[66] M.L. Brader, E.W. Ainscough, E.N. Baker, A.M. Brodie, S.L. Ingham, J. Chem. Soc. Dalton Trans. (1990) 2785.
[67] E.W. Ainscough, A.M. Brodie, R.J. Cresswell, J.C. Turnbull, J.M. Waters, Croat. Chem. Acta 72 (1999) 377.
[68] J.V. Hanna, M.E. Smith, S.N. Stuart, P.C. Healy, J. Phys. Chem. 96 (1992) 7560.
[69] L.L. Cheruiyot, L.K. Thompson, J.E. Greedan, G. Liu, R.J. Crutchley, Can. J. Chem. 73 (1995) 573.